KSME

Springer

Journal of Mechanical Science and Technology 34 (4) 2020

**Original Article**
DOI 10.1007/s12206-020-0313-2

**Keywords:**
· CFRC
· Finite element analysis
· Delamination
· FLSC

**Correspondence to:**
Rong Chen
r_chen@nudt.edu.cn

**Citation:**
Sun, J., Ma, Z., Zhang, Z., Weng, F., Chen, R. (2020). The delamination of carbon fiber reinforced composites during cutting by flexible linear shaped charge. Journal of Mechanical Science and Technology 34 (4) (2020) 1515~1522. http://doi.org/10.1007/s12206-020-0313-2

Received June 26th, 2019
Revised December 23rd, 2019
Accepted February 3rd, 2020

† Recommended by Editor Chongdu Cho



# The delamination of carbon fiber reinforced composites during cutting by flexible linear shaped charge

**Jing Sun[1], Zhiguo Ma[2], Zhifeng Zhang[1], Fei Weng[3] and Rong Chen[4]**

[1]Beijing Institute of Astronautical Systems Engineering, Beijing 100076, China, [2]Nanjing Research Institute of Simulation Technology, Nanjing 210000, China, [3]Department of Engineering Mechanics, Dalian University of Technology, Dalian 116024, China, [4]College of Liberal Arts and Sciences, National University of Defense Technology, Changsha 410073, China

**Abstract** The delamination is a typical phenomenon when the carbon fiber reinforced composites (CFRC) undergoes blasting impact loading and the delamination will reduce both the strength and stiffness of the laminates, which can lead to catastrophic consequences while used as rocket skin. In this paper, the response of CFRC laminate is cut by flexible linear shaped charge (FLSC) and the delamination behavior of the CFRC is analyzed and discussed. The displacement interferometer system for any reflector (DISAR) is used to monitor the velocity of characteristic points of the laminate subjected to FLSC. Finite element analysis has been conducted to explain the mechanisms of delamination. Based on the numerical simulation, the influences of structural design parameters on the delamination effect of the CFRC after cutting are investigated. The results show that a large number of debris are produced at the center of the explosion and a small amount of large debris is produced at weakening groove on both sides. The delamination effect is greatly affected by the inter-laminar tensile strength and thickness of composite laminate, but it is not significantly affected by the linear density of the FLSC and stand-off.

## 1. Introduction

Due to the superior strength and stiffness, CFRC are widely used in various field, such as vehicles, patrol boats and crafts in both military and civilian platforms. With the development of space carrying technology, these advanced structures requires high specific strength [1, 2]. Therefore, CFRC is widely used in the structure of rocket due to its advantages of high mass-specific strength and modulus [3].

Pyrotechnic devices such as the mild detonating fuse (MDF) and FLSC are used to perform releasing, cutting and other mechanical work for the separation of subsystems, boosters, stages, or payload satellites [4]. When CFRC structures are employed in the rocket skin, weakening grooves cannot be directly used due to strength design which is reasonable for MDF devices. Furthermore, the delamination effect of CFRC can lead to further damage of the rocket. One solution in structure design is to employ additional metal structure for the separation purposes only, however, this brings in an obvious penalty of weight and complexity in the design. The primary problem for the explosive cutting method (such as FLSC) of composite shells is that adjacent structures or materials fails in the cutting, which weakens the strength and stiffness of the composites and the fragments caused by the material fracture will change the flight path.

In recent years, a number of investigations have been conducted on the delamination of composite materials, which mainly focused the effect of explosions or blasts on delamination [5, 6]. Mouritz et al. [7] investigated the dynamic response of glass-fiber-reinforced composites structures to underwater blast loads. They found that blast can result in matrix cracking, delamination and fiber fracture of composites structures, and the combined effect significantly

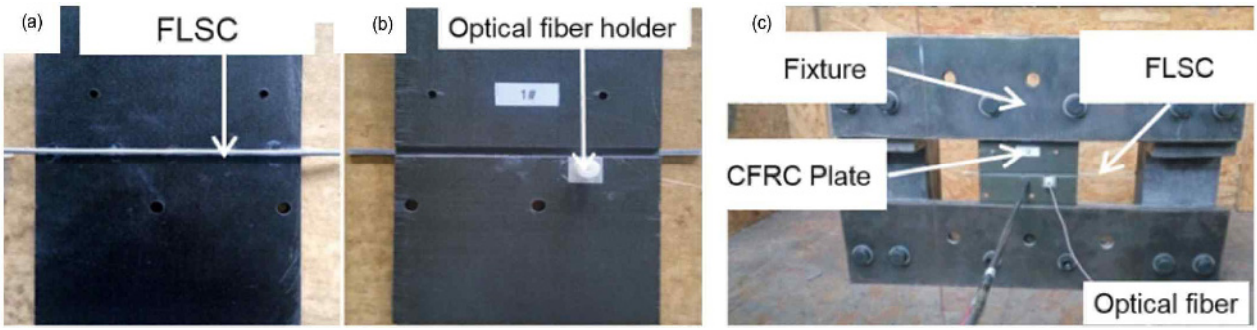


Fig. 1. Details of the experiment: (a) The FLSC is glued on the CFRC laminate; (b) the fiber holder to measure the off surface partial velocity; (c) the CFRC laminate is fixed by the fixture.

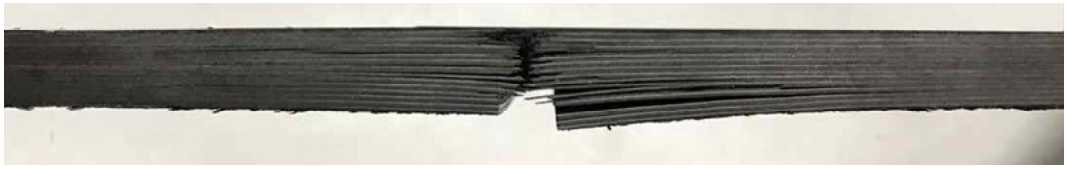

Fig. 2. CFRC laminate cut by FLSC.

reduced the load-bearing ability of the composite structure. Yahya [8] investigated the blast resistance of a carbon fiber-reinforced epoxy resin. For the cutting process of linear shaped charge, the main effect is caused by the high speed jet with the speed up to 7000 m/s which is much higher than that of an abrasive jet [9]. Batra and Hassan reported an in-house developed, three-dimensional finite element code, with rate dependent damage evolution equations for anisotropic bodies, and used the code to numerically ascertain the damage developed in a fiber-reinforced composite due to shock loads representative of those produced by an underwater explosion [10]. The main problem in the CFRC cutting includes non-even cutting surface, critical delaminate and side fragments. Therefore, it is significant to study the impact of explosion during the cutting of CFRC laminates.

In this paper, the cutting test and numerical model calculation is used to explore the dynamic response of laminates under the action of FLSC. In particular, the DISAR method is used to verify the rationality of the finite element model. In addition, the investigation of delamination of the CFRC laminate during the cutting by FLSC is focused. The influences of structure design parameter on the delamination of the CFRC during cutting are analyzed and discussed.

## 2. Method

### 2.1 Experimental setup

The composite laminate is made of carbon fiber from different angles with the dimension of 170 mm×125 mm, and the thickness of the laminate is 5 mm. The composite laminate is made from carbon fiber and bismaleimide resin. The laminate is laid out in a laminated form by a unidirectional material according to a predetermined fiber direction and order, and then bonded, and formed by heat curing. The laying method of the test laminates is $[\pm45/90/0/(\pm45)_4/0]_s$. The thickness of the each layer of CFRP composite laminate is about 0.15 mm. The laminates of different thicknesses are appropriately increased or decreased according to the above-mentioned laying manner.

The FLSC is a continuous hexogen (RDX) core enclosed in a seamless metal sheath that is made of lead antimony alloy. The cutting principle of the LSC can be summarized as follows: When the explosive is detonated, the metal cover is pressed and under high pressure of up to tens of millions KPa generated by the explosion and closed to the axis of symmetry. Then the high-speed collision occurs in the plane of symmetry, so that the metal near the inner wall of the cover is extruded on the plane of symmetry to form the jet which is often referred to as the "jet knife" and its head speed is several km/s. Under such high speed and high pressure, the target is cut into two. Charges are shaped in the form of an inverted “V” allowing the continuous metal sheath liner and encased explosive to produce a uniform linear cutting action upon detonation. The linear density of RDX is 3.0 g/m. The FLSC is glued on the laminate to ensure that the FLSC is not bent at the cutting surface. The stand-off of the FLSC is 0 mm.

The DISAR [11] is used to measure the surface velocity of the laminated plate, as shown in Fig. 1(b). DISAR requires that the test surface should be flattened to reflect the laser, while the carbon fiber composite laminate has a rough surface and the color is dark and does not meet the test conditions. In this paper, the aluminum foil is attached to the surface of the laminate to reflect the laser.

The FLSC is detonated from one side by an electric detonator. The laminate is clamped on both sides of the laminate to prevent splitting of the structure, as shown in Fig. 1(c). The laminate subjected to FLSC is shown in Fig. 2. There are obvi-

Table 1. Material parameters of RDX [13].

| $\rho_0$ (g/cm$^3$) | $D$ (m/s) | $P_{cj}$ (GPa) | $A$ (GPa) | $B$ (GPa) | $R_1$ | $R_2$ | $\omega$ | $E_0$ (GPa) |
|---|---|---|---|---|---|---|---|---|
| 1.82 | 7500 | 39.3 | 778.3 | 7.071 | 4.2 | 1.0 | 0.34 | 8.5 |

Table 2. Material parameters of unidirectional laminate [13].

| $\rho_0$ (g/cm$^3$) | $E_a$ (GPa) | $E_b$ (GPa) | $v_{ba}$ | $G_{ab}$ (GPa) | $G_{bc}$ (GPa) | $G_{ca}$ (GPa) | $X_c$ (GPa) | $X_t$ (GPa) | $Y_c$ (MPa) | $Y_t$ (MPa) | $S_c$ (MPa) |
|---|---|---|---|---|---|---|---|---|---|---|---|
| 1.80 | 148 | 10.3 | 0.02 | 6.02 | 93.31 | 6.02 | 1.53 | 1.92 | 255 | 56 | 90.5 |

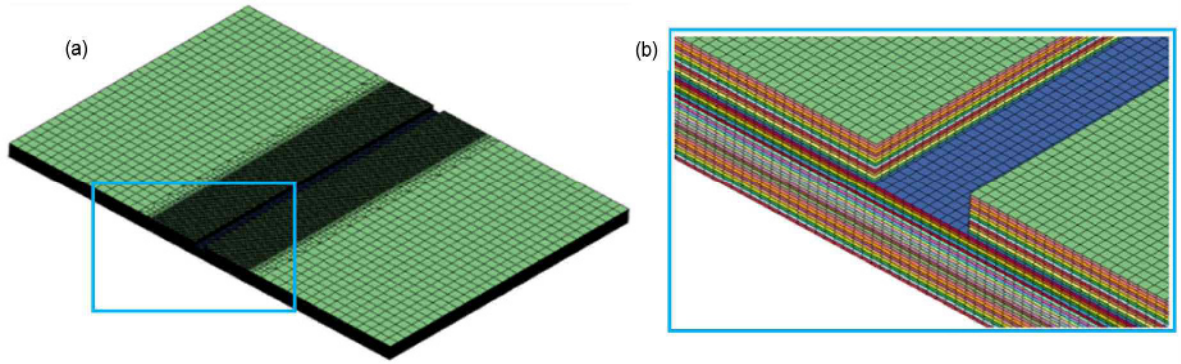


Fig. 3. Finite element model of CFRC laminates: (a) Whole laminate model; (b) local magnification of laminate model and the groove.

ous tearing, debris and delamination near the cutting surface.

## 2.2 Numerical model

In order to further study the damage mode and the influence of structural parameters on the delamination of the CFRC laminates under the explosive impact of FLSC, the finite element model (FEM) of CFRC laminates is established the same as the experimental setup, as shown in Fig. 3.

In this paper, the coupled Euler Lagrange (CEL) algorithm is adopted in the finite element dynamic calculation (LS-DYNA) [12] to evaluate the failure process of CFRC subjected to the explosive impact of FLSC. The composite laminates in the model are meshed into Lagrange elements, the FLSC and the surrounding air regions are set as Eulerian elements. The combined region of the two elements is a mixed Lagrange-Eulerian element region.

The material of *MAT_HIGH_EXPLOSIVE_BURN, and JWL equation of state are used to simulate the performance of RDX in FLSC, the parameters are shown in Table 1 [13]. The material model of *MAT_LAMINATED_COMPOSITE FABRIC is used to simulate the composite laminate [12]. Each layer is defined by the *SECTION_SHELL keyword according to the actual laying of the composite laminates. Material parameters of unidirectional laminate are shown in Table 2 [13]. The thickness of each layer is 0.15 mm, the number of the composite material layer can increase or decrease depending on the thickness of the composite laminates under different conditions.

The overall structure of the composite laminate is defined by the material parameters and direction of every single layer, and then equivalent the interaction between the layers of the composite laminate by defining the contact between the layers. The contact keyword used is *CONTACT_AUTOMATIC_SURFACE_TO_SURFACE_TIEBREAK. This key word determines whether to cancel the initial fixed contact by defining the tensile strength $\sigma_{NFLS}$ and the shear strength $\sigma_{SFLS}$ between the layers and thus simulate the delamination of the composite laminate. A fixed failure criterion (OPTION = 2) based on the Hoffman strength criterion is used, as shown in Eq. (1) [12].

$$\left(\frac{|\sigma_n|}{\sigma_{NFLS}}\right)^2+\left(\frac{|\sigma_s|}{\sigma_{SFLS}}\right)^2\geq 1 \tag{1}$$

In which, the $\sigma_{NFLS}$ is inter-laminar tensile strength and the $\sigma_{SFLS}$ is inter-laminar shear strength.

## 2.3 Model validation

The velocity history of the surface characteristic position in z-direction (perpendicular to the surface of the laminate) is shown in Fig. 4. There are two stages in the velocity curve. The first stage is the wave propagation process in the range of 0 to 30 μs and the second stage is the warping process of the laminated plate after 30 μs. In the wave propagation process, the detonation wave arrives the FLSC corresponding to the measuring point 11 μs after the initiation. The measuring point is 100 mm away from the detonator and the detonation velocity is 7500 m/s. The trigger starts timing from about 2.5 μs after initiation. The detonation wave reaches the measuring point at

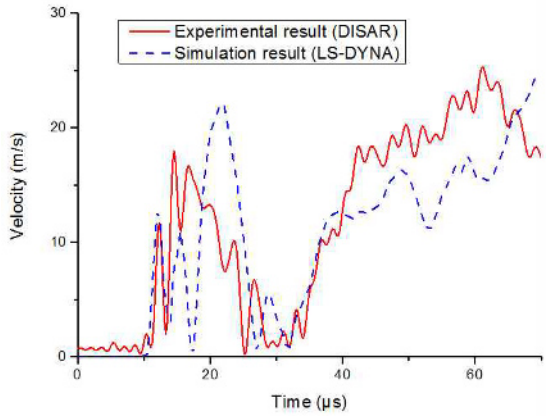


Fig. 4. Z-velocity of characteristic position.

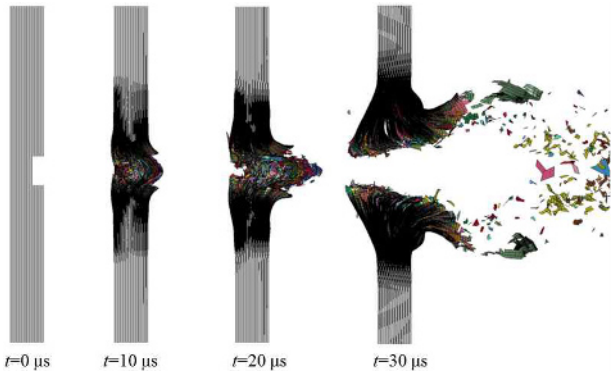


Fig. 5. Failure process of composite laminate.

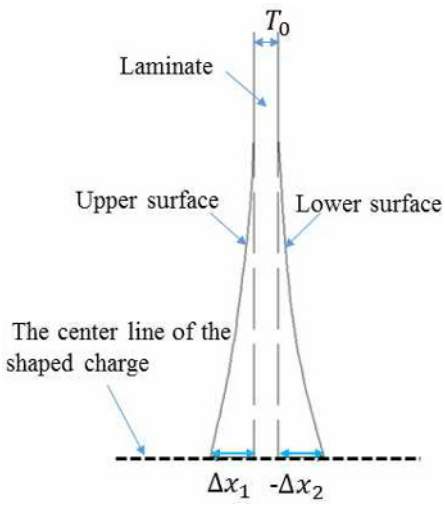


Fig. 6. The principle of evaluating delamination ratio ε of the laminate.

10.9 μs. The first extreme value of 12.69 m/s arrives at 12.0 μs corresponding to the first shock wave. The corresponding experimental result is 11.72 m/s at 12.3 μs which is consistent with the modeling results. The velocity gradually fluctuates to the maximum value in the following 10 μs. The velocity of the characteristic position will decrease to zero at about 30 μs and then gradually increase again. In addition, the maximum velocity of the test and simulation in 0-30 μs is 17.6 m/s and 22 m/s, and the error is 12 %. What's more, the curve trends of the test and simulation are consistent at this stage despite the existence of non-negligible stress wave effects. The DISAR joint has been separated from the laminate after 70 μs and the differences of the velocity history can be ignored of the subsequent time. This means that the numerical and experimental velocity curves of the characteristic position are basically the same, which validates the credibility of the simulation results.

## 3. The delamination damage during cutting

The failure process of the CFRC laminate after the detonation of the FLSC is shown in Fig. 5. The energy of the FLSC is applied on the groove and the surrounding areas, the laminate is deformed as a whole part and the local inter-laminar connections fail. When the cutting surface is completely separated, the inter-laminar connection in the area near cutting surface is largely defective, the delamination is serious and the fragments of carbon fiber flakes are produced.

In addition, the damage of composite laminate mainly concentrates in the distance less than 20 mm from the groove, the width of the complete destroyed area is between 1-2 mm, the delamination happened near to the cutting area and almost no damage happens in the far filed. A large number of small pieces are produced at the cutting area and a small amount of large debris is also produced at the surface of composite laminate groove on both sides. The damaged area and shape are basically consistent with the test results (shown in Fig. 2).

In order to evaluate the degree of delamination damage of composite laminate, the delamination ratio $\varepsilon$ is used to characterize the delamination of the composite laminate in the thickness direction. The principle of evaluating delamination ratio $\varepsilon$ of the laminate is shown in Eq. (2) and Fig. 6. The $T_0$ is the original thickness of the laminate, $\Delta x_1$ and $\Delta x_1$ the displacement difference of characteristic points of upper and lower surfaces of the laminate respectively.

$$\varepsilon = \frac{|\Delta x_1 - \Delta x_2|}{T_0} \tag{2}$$

Ten sets of characteristic point are extracted from the upper and lower surfaces along the center line of shaped charge by the distance of 13 mm-22 mm ($d$), and the mean value of each group of characteristic points is calculated. Fig. 7 shows the distribution of characteristic points and the dotted area is characteristic points region of evaluating the $\varepsilon$ of the laminate.

## 4. Effect of structural parameters on the delamination of laminates

### 4.1 Effect of linear density of the FLSC on the delamination

The linear density ($\rho_l$) of the FLSC directly determines the amount of energy released during the explosion cutting of the laminate, which affects the impact on the composite laminate.

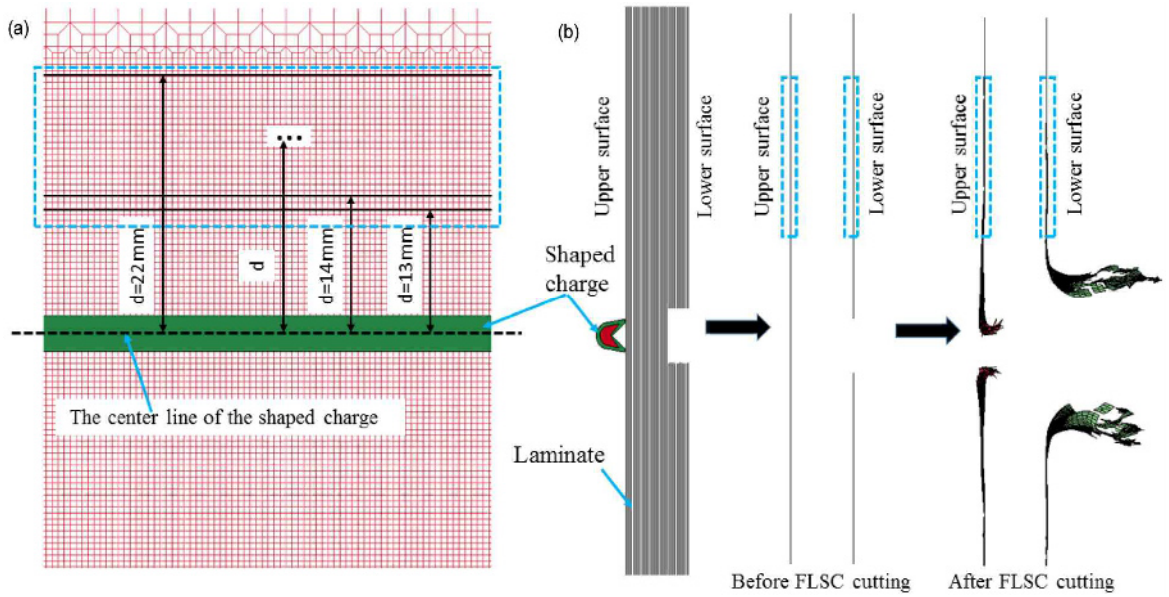


Fig. 7. Distribution of characteristic points: (a) Front view of the laminate; (b) side view of the laminate.

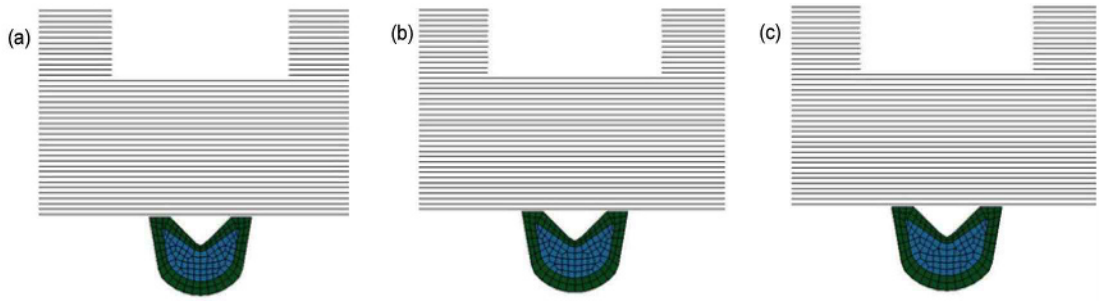


Fig. 8. FEM with different linear density of the FLSC: (a) $\rho_l$ = 3.5 g/m; (b) $\rho_l$ = 3.85 g/m; (c) $\rho_l$ = 4.2 g/m.

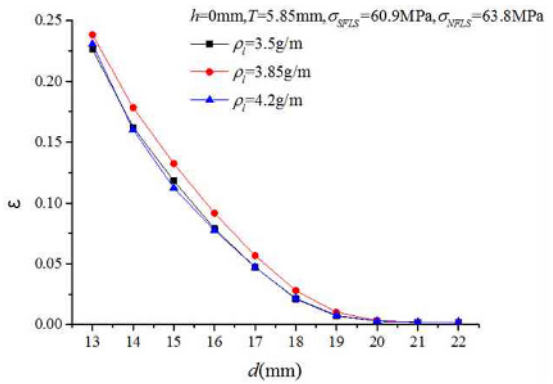


Fig. 9. The delamination ratio ε of the laminate for different linear density of the FLSC.

Therefore, three conditions ($\rho_l$ = 3.5, 3.85 and 4.2 g/m) are designed as shown in Fig. 8. The delamination ratio ε of the laminate in each condition is statistically analyzed in Fig. 9.

It is clear that under the conditions of *d* in the range of 13 mm-20 mm, the difference in delamination is small under different linear density conditions. Therefore, the influence of linear density on the delamination of composite laminate is not obvious when the linear density of FLSC is 3.5 g/m ≤ $\rho_l$ ≤ 4.2 g/m.

## 4.2 Effect of stand-off on the delamination

In the case of general impact damage, the distance between the impact source and the target, named as the stand-off (*h*), is an important factor affecting the degree of delamination of the laminate. Therefore, the delamination ratio of composite laminate for three different stand-off conditions are analyzed, which are 0, 0.5 and 1.0 mm, respectively as shown in Fig. 10.

The distribution of the delamination ratio ε at the characteristic point with the distance to the FLSC influenced by different stand-off is shown in Fig. 11. When *d* is in the range of 13 mm~16 mm, for the 1.0 mm stand-off, delamination level is less than the other two conditions. The maximum rate of the ε is controlled at 10 %. While the three conditions have no difference in case of delamination when *d* is in the range of 17 mm~22 mm. Therefore, it can be concluded that the stand-off has no critical effects on the degree of delamination of the composite laminate when the stand-off changes from 0 mm to 1.0 mm.

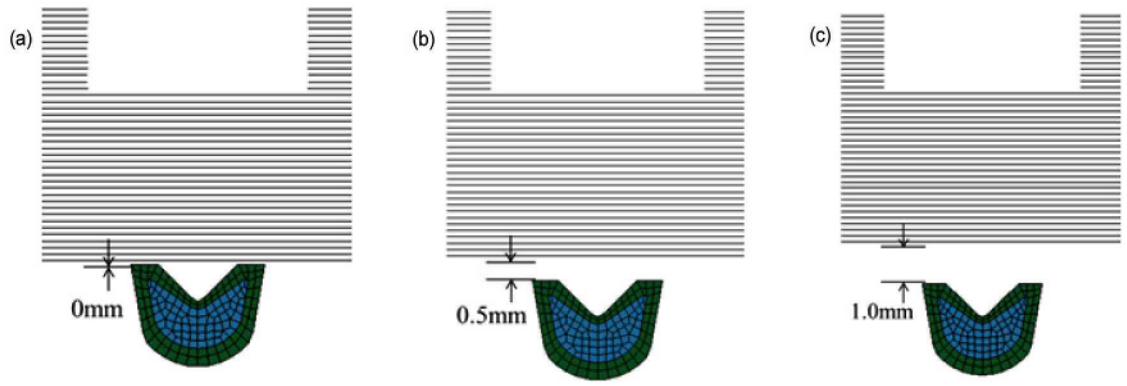


Fig. 10. FEM with different stand-offs: (a) h = 0 mm; (b) h = 0.5 mm; (c) h = 1.0 mm.

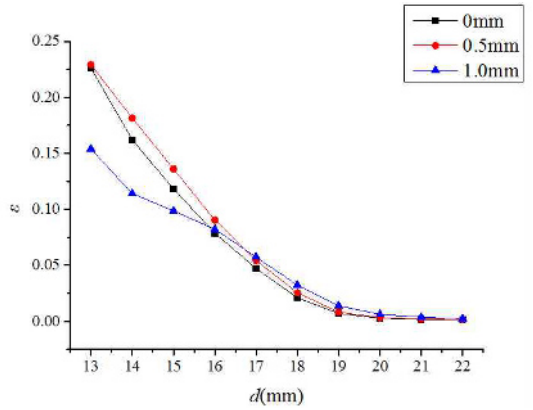


Fig. 11. The ε of the laminate for different stand-offs.

### 4.3 Effect of thickness of laminate on the delamination

The delamination ratio of the composite laminate is also affected by the thickness of the laminate. Three different thickness ($T$) conditions are designed, which are 5.85 mm, 6.75 mm and 7.65 mm, and there are 39, 45 and 51 single layers respectively as shown in Fig. 12. The thickness of each layer is 0.15 mm and the thickness of the groove is 1.95 mm.

The distribution of the delamination ratio $\varepsilon$ at the characteristic point with the distance to the FLSC influenced by different laminate thicknesses is shown in Fig. 13. When $d$ is in the range of 13 mm-20 mm, compared with the other two condition, the delamination ratio $\varepsilon$ of the composite laminate reaches the maximum value under $T$ = 5.85 mm. When $d$ is in the range of 13 mm-14 mm, the $\varepsilon$ of the composite laminate under $T$ = 7.65 mm is larger than that of $T$ = 6.75 mm. While the $\varepsilon$ of composite laminate under $T$ = 6.75 mm is larger than that of $T$ = 7.65 mm working conditions for the range of 14 mm~20 mm. It is obvious that the thickness of the laminate has a significant effect on the delamination of the composite laminate.

### 4.4 Effect of interlaminar tensile strength on the delamination

In the case of inter-laminar tensile strength, the tensile strength of $\sigma_{NFLS}$ = 63.8, 57.4 and 51.0 MPa are considered, and the other parameters for simulating calculation of CFRC are the same. The delamination ratio $\varepsilon$ of characteristic points in the thickness direction of the composite laminate are calculated for different inter-laminar tensile strength as shown in Fig. 14.

It is obvious that there is almost no delamination occurs outside 22 mm of the FLSC. As the distance decrease, the delamination of CFRC is more serious. Comparing different inter-laminar tensile strength, in the case of $\sigma_{NFLS}$ = 63.8 MPa, the maximum delamination distance of the laminate is 20 mm. When the $\sigma_{NFLS}$ = 57.4 MPa and $\sigma_{NFLS}$ = 51.0 MPa, the maximum delamination distance of the laminate is 21 mm and 22 mm respectively. At the same distance ($d$), the delamination of composite laminate increases with the decrease of inter-laminar tensile strength. What's more, the delamination ratio for $\sigma_{NFLS}$ = 51.0 MPa is largest, the delamination ratio is second when $\sigma_{NFLS}$ is 57.4 MPa, and the delamination ratio is smallest in $\sigma_{NFLS}$ = 63.8 MPa working condition. In addition, when the distance $d$ between characteristic point and the FLSC changes within a small range, the delamination ratio $\varepsilon$ changes linearly. When it changes in a large range, the delamination ratio $\varepsilon$ changes non-linear. It is clear that the interlaminar tensile strength is an important factor affecting the delamination effect of CFRC.

## 5. Conclusion

The dynamic response of the CFRC laminates subjected to the FLSC is investigated by means of both experiments and numerical modeling. The DISAR is used to monitor the velocity of surface characteristic point of the laminate. In terms of cutting velocity, the simulation results and the experimental results are agrees with each other, and the error of the size is also within reasonable range, which validates the feasibility of the simulation method. The influence of multiple structural parameters on the delamination phenomenon is analyzed and the following conclusions can be obtained:

(1) The results show that the delamination damage of CFRC laminates mainly concentrates within 22 mm from the center line of FLSC.

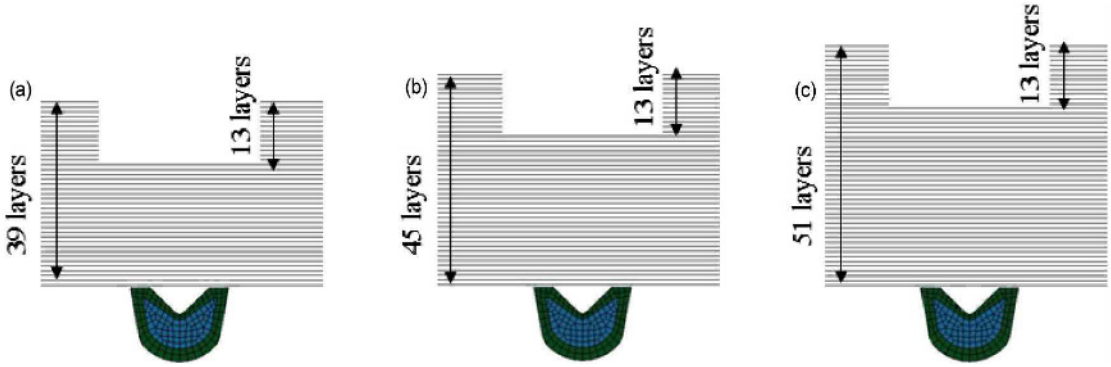


Fig. 12. FEM with different laminate thickness: (a) $T$ = 5.85 mm; (b) $T$ = 6.75 mm; (c) $T$ = 7.65 mm.

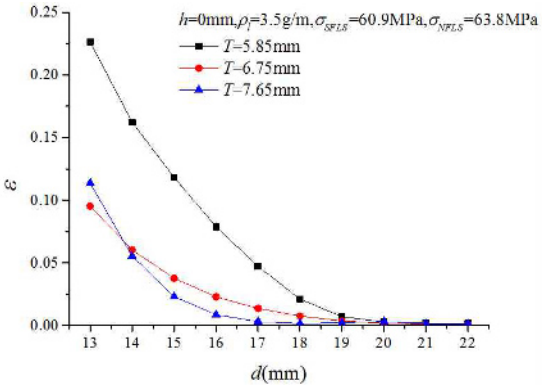


Fig. 13. The delamination ratio $\varepsilon$ of the laminate for different laminate thicknesses.

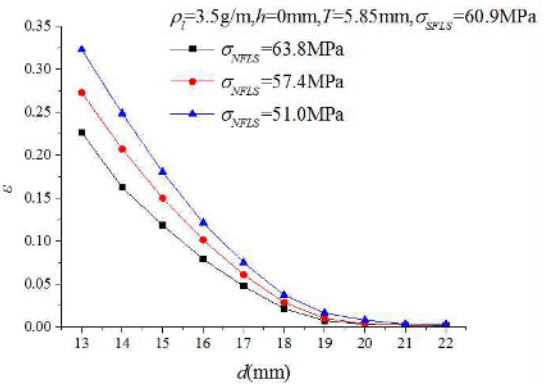


Fig. 14. The delamination ratio $\varepsilon$ of the laminate for different inter-laminar tensile strength.

(2) The failure of composite laminate changes with the distance to the FLSC. There is a complete destruction area at the FLSC that produces a large number of small pieces; delamination happens near the FLSC, and a small amount of large debris was also produced at the weakening groove on both sides. No damage occurs far away from the cutting area.

(3) The inter-laminar tensile strength and thickness of composite laminate are important factors influencing the delamination of the composite laminate. In a certain range, the linear density of the FLSC and stand-off have no critical influence on the delamination ratio of composite laminate.

## Acknowledgements

This wok was financially supported by National Natural Science Foundation of China [grant no. 11602030 &11672328].

## References

[1] S. F. Hwang et al., Progressive failure of metal–composite hybrid wheels under impact, *Journal of Mechanical Science and Technology*, 32 (1) (2018) 223-229.

[2] J.-K. Choi, K.-S. Park and S.-S. Lee, Predicting the hardening depth of a sprocket by finite element analysis and its experimental validation for an induction hardening process, *Journal of Mechanical Science & Technology*, 32 (3) (2018) 1235-1241.

[3] C. Tao et al., Dynamical model and experimental study of low-shock separation device, *Astronautical Systems Engineering Technology* (2017).

[4] K. E. Konno, D. A. Catalano and T. M. Krivanek, Evaluation of separation mechanism design for the orion/ares launch vehicle, *Proceedings of the 39th Aerospace Mechanisms Symposium* (2008).

[5] A. P. Mouritz, Ballistic impact and explosive blast resistance of stitched composites, *Composites. Part B*, 32 (5) (2001) 431-439.

[6] M. Y. Yahya et al., The blast behavior of fiber reinforced thermoplastic laminates, *Journal of Composite Materials*, 42 (21) (2008) 2275-2297.

[7] A. P. Mouritz, D. S. Saunders and S. Buckley, The damage and failure of GRP laminates by underwater explosion shock loading, *Composites*, 25 (6) (1994) 431-437.

[8] M. Y. Yahya et al., The blast resistance of a woven carbon fiber-reinforced epoxy composite, *Journal of Composite Materials*, 45 (7) (2011) 789-801.

[9] N. D. Parab and W. W. Chen, Crack propagation through interfaces in a borosilicate glass and a glass ceramic, *International Journal of Applied Glass Science*, 5 (4) (2014) 353-362.

[10] R. C. Batra and N. M. Hassan, Response of fiber reinforced composites to underwater explosive loads, *Composites Part B (Engineering)*, 38 (4) (2007) 448-468.

[11] J. Weng et al., Optical-fiber interferometer for velocity

measurements with picosecond resolution, *Applied Physics Letters*, 89 (11) (2006) 111101.

[12] *LS-DYNA Version 971 Keyword User's Manual*, CA: Livermore Software Technology Corporation (2012).

[13] M. Zhiguo, Research on impact fracture behavior of carbon fiber laminates under explosive of linear shaped charge, *Master's Thesis*, Changsha: Graduate School of National University of Defense Technology (2016).

**Jing Sun** is a senior engineer at the China Aerospace Science and Technology Corporation one institute. She is mainly engaged in structural strength analysis and pyrotechnic separation device design.